Nuclear Engineering and Technology 53 (2021) 3352–3358

Contents lists available at ScienceDirect

Nuclear Engineering and Technology

journal homepage: www.elsevier.com/locate/net

Original Article

Adsorption and separation behaviors of Y(III) and Sr(II) in acid solution by a porous silica based adsorbent

Hao Wu, Taiga Kawamura, Seong-Yun Kim*

Department of Quantum Science and Energy Engineering, Graduate School of Engineering, Tohoku University, Sendai, Miyagi, 980-8579, Japan

ARTICLE INFO

Article history:
Received 8 January 2021
Received in revised form
21 March 2021
Accepted 7 April 2021
Available online 24 April 2021

Keywords:
Separation
Yttrium
Strontium
Chromatography

ABSTRACT

Aiming at selective adsorption and separation of Y(III) from the Y(III)–Sr(II) group in acid solution, a silica-based TODGA impregnated adsorbent [(TODGA+1-dodecanol)/SiO_2–P–F600] has been prepared. Batch adsorption experiments were conducted under the effect of contact time, acid concentration, solution temperature, and adsorption capacity etc. Chromatography recovery of more than 90% Y(III) was successfully achieved under elution with 0.01 M DTPA solution in nitric acid adsorption system, and 0.1 M HCl solution in hydrochloride adsorption system, respectively.

1. Introduction

Yttrium-90 ($T_{1/2}$ = 67.4 h) as a strong β radiation emitter with a maximum energy of 2.28 MeV (average energy of 0.94 MeV) [1], can penetrate soft tissues up to 1 cm, possessing the properties of simple chemistry in solution and strong complexing affinity with numerous chelating agents, has been widely utilized in the field of radiopharmaceuticals, playing a significant role for various therapeutic applications [2,3]. Till now, two main methods have been developed for achieving ^{90}Y, one is produced by neutron bombardment of naturally occurring ^{89}Y, while extremely low specific activity in tracers was obtained because of its low activation cross section [4]. On the other hand, its separation from long-lived parent nuclide ^{90}Sr ($T_{1/2}$ = 28.8 y) generated in high-level liquid waste (HLLW) makes the continual supply of high purity ^{90}Y feasible by milking it at desired intervals [5]. Therefore, numbers of methods such as ion exchange, precipitation, solvent extraction, adsorption, membrane etc. have been reported about the separation of ^{90}Y from ^{90}Sr [6,7]. Due to the advantages of consumption of less organic solvents, less secondary wastes, no third phase formation, continuous operation etc., solid phase extraction (Adsorption) as the one of the most favorable methods, has attracted much attention for the practical utilization in the separation of ^{90}Y with ^{90}Sr [8,9]. And two strategies were commonly considered for selecting a suitable cheat agent used in chromatography separation process. Firstly, in the case of Sr, a crown ether compound has been previously reported as an effective extractant, while its expensive price was frustrating [10]. In the case of Y, numerous extractants, such as octyl(phenyl)-*N, N*-diisobutylcarbamoyl methylphosphine oxide (CMPO), *N,N,N'N'*-tetraoctyl diglycolamide (TODGA) etc., were reported to exhibit high affinity towards rare earth metals. T. Kawamura et al. studied the adsorption performance between Y and Sr by using a CMPO impregnated adsorbent in HNO_3 and HCl solutions [11]. Their results showed that the adsorbent had a high adsorption affinity of Y than Sr, and with an increase in the concentration of HNO_3, the maximum K_d value reached 100 when [HNO_3] = 5 M. While the K_d values of Y in HCl solution was found to be not high (<10). Comparing to CMPO, TODGA consisting of only C, H, N, O atoms, was reported to display more unique extraction behaviors, acted more efficient and environmental-friendly etc. On the other hand, the combination of TODGA with other agents was reported to exhibit characteristic enhancement in adsorption properties [12]. Therefore, the objective in this study mainly focused on preparation a porous silica-based adsorbent impregnating with TODGA (as chelating agent) and 1-dodecanol (as molecule modifier). And its adsorption and separation behaviors of Y and Sr will be evaluated in HNO_3 and HCl solution, respectively.

* Corresponding author.
E-mail address: sonyun.kimu.d7@tohoku.ac.jp (S.-Y. Kim).

https://doi.org/10.1016/j.net.2021.04.009

2. Experimental

2.1. Reagent

Strontium nitrate [$Sr(NO_3)_2$], Strontium chloride ($SrCl_2$), Yttrium nitrate hexahydrate [$Y(NO_3)\cdot 6H_2O$], Yttrium chloride hexahydrate (YCl_3), Diethylenetriaminepentaacetic acid (DTPA) etc. were purchased from FUJIFILM Wako Pure Chemical Corporation and were of analytical grade (>99%). All the aqueous solution used in this study were prepared in deionized distilled water with a specific resistance of 18.3 MΩ cm or greater. Porous silica particles (SiO_2–P–F600) with a mean particle size of ~50 μm and a mean pore size of ~600 nm were selected as support material [13]. The symbol "P" means styrene-divinylbenzene copolymer immobilized into the pores of silica support [14]. The selected ligand *N, N, N′, N′*-tetraoctyl diglycolamide (TODGA) and its molecular modifier 1-dodecanol were commercially available from Chemicrea Inc. and used directly without any further purification.

2.2. Synthesis procedures of (TODGA+1-dodecanol)/SiO_2–P–F600 adsorbent

On the basis of previous reports, the synthesis procedures of (TODGA+1-dodecanol)/SiO_2–P–F600 adsorbent could be briefly divided into two main steps [15,16]. Firstly, as many industrial organic impurities still remained in the pores of purchased silica particles (SiO_2–P–F600). The SiO_2–P–F600 particles should be washed by methanol several times until the filtrate became colorless and then dried in a vacuum for approximately 1 day. Secondly, 10 g of TODGA and 1-dodecanol (added as molecule modifier) were dissolved in 200 mL dichloromethane (CH_2Cl_2). 20g of dried SiO_2–P–F600 particles were then slowly added into the above solution. Above prepared mixture was carefully transferred to the EYELA OSB-2100 rotary evaporator (Tokyo Rikakikai Co. Ltd., Japan) and stirred mechanically for 1~2 h at room temperature. Then, with gradually increasing the temperature in water bath and decreasing the vacuum, CH_2Cl_2 was evaporated and TODGA was impregnated into the pores of SiO_2–P–F600 particles with 1-dodecanol. The residue of CH_2Cl_2 remained in pores was further removed following drying in a vacuum oven at 338 K for more than 24 h. Therefore, TODGA and 1-dodecanol could be evenly distributed into the pores of SiO_2–P–F600 particles. The morphology of prepared (TODGA+1-dodecanol)/SiO_2–P–F600 adsorbent was characterized by JEOL scanning electron microscope (SEM) JSM-6610LV with integrated energy dispersive X-ray analyzer (EDX) system. The pore textural properties of prepared adsorbent were measured on BELSORP-max adsorption apparatus (MicrotracBEL, Corp.) at 77 K.

2.3. Batch adsorption experiments

The adsorption performances of prepared (TODGA+1-dodecanol)/SiO_2–P–F600 adsorbent towards Y(III) and Sr(II) were conducted under the effect of contact time, acid concentration, solution temperature, adsorption capacity etc. In the experiments of the effect of contact time, effect of adsorption temperature, the aqueous phase containing 5 mM Y(III) and Sr(II) in 1 M HNO_3 and HCl were prepared. Contact time was changed from 10 min to 4 h. And experimental temperature was set as 288, 298, 308 and 323 K, respectively. In the experiments of the effect of acid concentration, the concentration of metal ions was still fixed as 5 mM, while the concentration of acid varied from 0.001 to 5 M. In the experiments of the effect of adsorption capacity, the concentration of metal ions was adjusted from 1 mM to 100 mM with a fixed acid concentration as 1 M. Next, 0.2 g of (TODGA+1-dodecanol)/SiO_2–P–F600 was weighted as solid phase mixing with 4 mL of above prepared working solutions in a 13.5 mL glass vial with a plastic cap. Two phases were completely mixed at 160 rpm for certain contact time under given temperature. Followed phase separation procedure was carried out using syringe setting up with a nylon net filter (20–40 μm pores). The concentration of Y(III) and Sr(II) before and after adsorption process were measured three times independently by inductively coupled plasma atomic emission spectrometer (ICP-AES, Shimazu ICPS-7510). The uptake percentages (E, %), adsorbed amount (Q, mmol/g), and distribution coefficient (K_d) of the tested Y(III) and Sr(II) by (TODGA+1-dodecanol)/SiO_2–P–F600 were calculated using the following equations [17,18].

$$E = \frac{C_0 - C_t}{C_0} \times 100 \quad (1)$$

$$K_d = \frac{C_0 - C_e}{C_e} \times \frac{V}{m} \quad (2)$$

$$q = (C_0 - C_t) \times \frac{V}{m} \quad (3)$$

where, C_0, C_t, C_e represent the concentration of Y(III) and Sr(II) in the aqueous phase (mM) at the initial, certain time and equilibrium state, respectively. m and V indicate the weight of dry (TODGA+1-dodecanol)/SiO_2–P–F600 (g) and the volume of the aqueous phase used (mL), respectively.

2.4. Chromatography separation experiments

5 mL of aqueous solutions containing 5 mM Y(III) and Sr(II) in 1 M acid solution were prepared as the feed solution using in chromatography separation experiments. Around 5 g of (TODGA+1-dodecanol)/SiO_2–P–F600 was packed into a glass column with the size of H 150 mm × Φ 8 mm by wet packing method. The thermo jacket covered outside the column can maintain the working temperature as the stable 298 K by circulating the thermostated water through an EYELA NCB-1200 equipment (Tokyo Rikakikai Co. Ltd., Japan). Flow rate was adjusted to the constant value of 0.3 cm^3/min 10 mL of 1 M HNO_3/HCl, 30 mL of 0.1 M HNO_3/HCl and 40 mL 0.01 M DTPA solution were sequentially flowed into the column as eluent. The effluent flowed out from glass column was automatically collected with each fraction of around 3 cm^3 aliquot by EYELA fraction collector DC-1500 [19]. The concentration of Y(III) and Sr(II) remained in effluent were measured in the same way with in batch experiments.

3. Result and discussion

3.1. Characterization

SEM and EDX characterizations of synthesized (TODGA+1-dodecanol)/SiO_2–P–F600 adsorbent was presented as shown in Fig. 1. It was found that (TODGA+1-dodecanol)/SiO_2–P–F600 adsorbent had a relatively smooth surface, suggesting that TODGA and 1-dodecanol had been successfully impregnated into the pores of SiO_2–P–F600 particle. On the other hand, EDX mapping revealed that the prepared (TODGA+1-dodecanol)/SiO_2–P–F600 adsorbent was consisted of the main element of C, O, Si, which was consistent with the composition of TODGA, 1-dodecanol, and SiO_2–P–F600. In addition, textural properties of SiO_2–P–F600 and prepared (TODGA+1-dodecanol)/SiO_2–P–F600 adsorbent were summarized as shown in Table 1, it could be found that before and after impregnation process, the average pore size decreased at some extent, indicating that TODGA and 1-dodecanol were

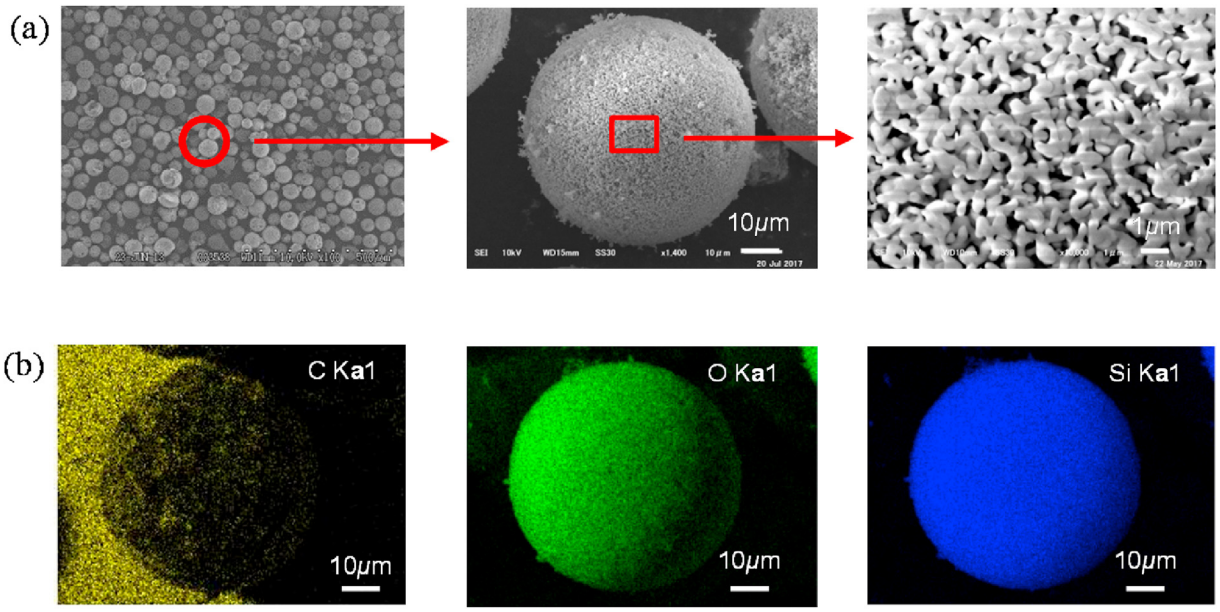

Fig. 1. (a) SEM images and (b) EDX mapping of prepared (TODGA+1-dodecanol)/SiO_2–P–F600 adsorbent.

Table 1
Summary of textural properties of SiO_2–P–F600 and prepared (TODGA+1-dodecanol)/SiO_2–P–F600 adsorbent.

	Average pore size (nm)	Total pore volume (cm^3/g)	Specific surface area (m^2/g)	SiO_2 (wt%)	TODGA+1-dodecanol (wt%)	SDB polymer (wt%)
SiO_2–P–F600	600	–	–	86.3	–	13.7
Adsorbent	16.01	0.004	1.073	43.2	50.0	6.8

accommodating into the pores of SiO_2–P–F600 support, not just adhering on its surface. And the compacted structure of prepared (TODGA+1-dodecanol)/SiO_2–P–F600 adsorbent is beneficial for its utilization in chromatography separation experiments.

3.2. Effect of contact time

The effect of contact time on Y(III) adsorption by (TODGA+1-dodecanol)/SiO_2–P–F600 adsorbent in 1.0 M HNO_3 and HCl solution were respectively carried out by varying the time intervals from 10 min to 4 h at 298 K and the obtained experimental results were illustrated as shown in Fig. 2. It was found that the adsorption rate was fairly fast at the very first beginning from 10 min to 1 h.

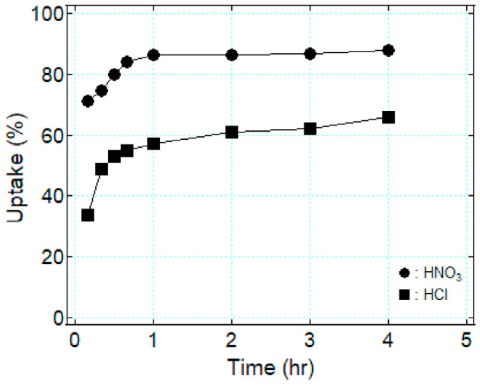

Fig. 2. Relationship between uptake percentage of Y(III) and contact time onto (TODGA+1-dodecanol)/SiO_2–P–F600 adsorbent at 298 K [Y(III)] = 5 mM; V/m = 20 cm^3/g; [HNO_3] or [HCl] = 1 M.

Then adsorption rate gradually slowed down and the uptake percentages were almost no significant change after 2 h with further increasing contact time in HNO_3 solution, indicating the adsorption process reached to an equilibrium state, no more Y(III) were further transferred from aqueous phase to (TODGA+1-dodecanol)/SiO_2–P–F600 adsorbent. While in HCl solution, it still has not reached equilibrium. And the differences in the time required to reach equilibrium state in HNO_3 and HCl solution were considered to be ascribed to the relatively weaker complexation ability of TODGA towards Y(III) with Cl^- ion as compared to that with NO_3^- ion [20]. On the other hand, the relatively slow adsorption rate in both HNO_3 and HCl solution was attributed to the porous structure of (TODGA+1-dodecanol)/SiO_2–P–F600 adsorbent. Y(III) was firstly transferred to the exterior surface of the (TODGA+1-dodecanol)/SiO_2–P–F600 particles under vigorous shaking speed and then gradually diffused into its pores, and finally captured by functional TODGA units. Therefore, all of the other adsorption experiments conducted in this study were performed by shaking for 5 h, which was considered to be long enough to reach the constant state.

In order to have a better understanding of the adsorption process of (TODGA+1-dodecanol)/SiO_2–P–F600 adsorbent towards Y(III) in 1 M HNO_3 and HCl solution, the widely used pseudo-second order kinetic model was selected to evaluate the obtained experimental data, and its linear expression was described as follows [21].

$$\frac{t}{q_t} = \frac{1}{k_2 q_e^2} + \frac{t}{q_e} \tag{4}$$

where, q_e and q_t mean the adsorption amount onto (TODGA+1-dodecanol)/SiO_2–P–F600 adsorbent at equilibrium state and at

time t, respectively (mg/g), k_2 (g/(mg·h)) is the rate constant of the second order at the equilibrium state.

Based on previous studies, it was well-known that pseudo-second order model assumed that adsorption rate was controlled by chemical adsorption process and its corresponding adsorption capacity was proportional to the number of active points on the adsorbent [22]. The kinetic data of t/q_t versus t for Y(III) adsorption were plotted as depicted in Fig. 3 and the calculated kinetic parameters of adsorption amount, rate constant, correlation coefficients were summarized as shown in Table 2. Obtained high correlation coefficient (>0.99) and proximity of calculated adsorption amount with experimental results indicated that the experimental data was in a good accordance with pseudo-second order model. For instance, the adsorption process explained as a chemisorption was feasible in both HNO_3 and HCl solution.

3.3. Effect of acid concentration

The effect of acid concentration on the adsorption performances of (TODGA+1-dodecanol)/SiO_2–P–F600 adsorbent towards Y(III) and Sr(II) were investigated in [HNO_3], [HCl] = 0.001–5 M, respectively and the results were summarized as shown in Fig. 4. Overall, (TODGA+1-dodecanol)/SiO_2–P–F600 adsorbent exhibited poor affinity (<10%) towards Sr(II) in both HNO_3 and HCl solution. On the other hand, in the case of Y(III), its uptake percentage increased gradually with increasing [HNO_3]. While when [HCl] increased from 0.001 to 0.1 M, the adsorption performance towards Y(III) remained stable. When [HCl] further increased from 0.1 to 5 M, its uptake percentage increased drastically to around 80%. The different adsorption behaviors of Y(III) using TODGA regarding to the concentration of acid in the solutions could be explained as the adsorption of Y(III) increased only when sufficient amount of acid and water were extracted to form TODGA aggregates [23]. And the obtained experimental tendency in HNO_3 and HCl solutions shown in Fig. 4 was consistent with previous reports [24]. Therefore, adsorption mechanism was attributed as Y(III) formed a complex with TODGA and HNO_3/HCl or even water molecules. The proposed complex formation equations were given as follows based on previous studies [25].

$$Y^{3+} + k(\text{TODGA+1-dodecanol})/SiO_2\text{–P–F600} + 3NO_3^- + nHNO_3 + mH_2O \leftrightharpoons Y[(\text{TODGA+1-dodecanol})/SiO_2\text{–P–F600}]_k(NO_3)_3(HNO_3)_n(H_2O)_m \quad (5)$$

$$Y^{3+} + z(\text{TODGA+1-dodecanol})/SiO_2\text{–P–F600} + 3Cl^- + xHNO_3 + yH_2O \leftrightharpoons Y[(\text{TODGA+1-dodecanol})/SiO_2\text{–P–F600}]_z(Cl)_3(HCl)_x(H_2O)_y \quad (6)$$

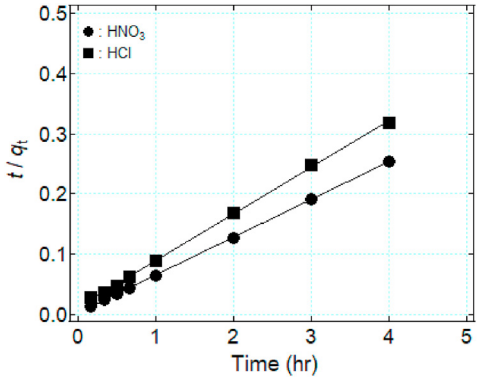

Fig. 3. Plot of the pseudo-second order model for Y(III) adsorption onto (TODGA+1-dodecanol)/SiO_2–P–F600 adsorbent.

Table 2
Summary for the fitting results of pseudo-second order kinetic model.

	K_2 (g/mg h)	Calculated q_e (mg/g)	Experimental q_e (mg/g)	R^2
HNO_3	1.597	15.934	15.740	1.000
HCl	0.504	12.926	12.566	0.999

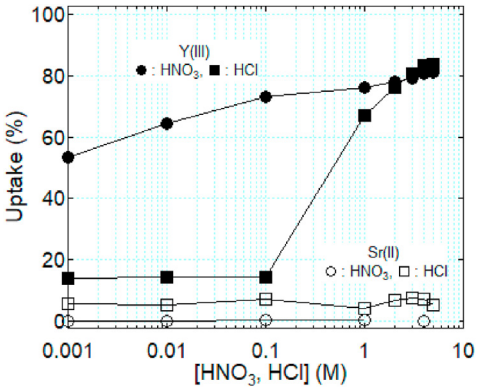

Fig. 4. Effect of acid concentration on uptake ratio of Sr(II) and Y(III) onto (TODGA+1-dodecanol)/SiO_2–P–F600 adsorbent at 298 K [Sr(II)], [Y(III)] = 5 mM; V/m = 20 cm^3/g; [HNO_3, HCl] = 0.001–5 M; shaking time: 5 h.

3.4. Adsorption capacity and isotherms

The adsorption capacity of (TODGA+1-dodecanol)/SiO_2–P–F600 adsorbent towards Y(III) in 1 M HNO_3 and HCl solution were also investigated respectively and the results were summarized as shown in Fig. 5. It was found that with increasing the initial concentration of Y(III) in aqueous phase, the adsorption amount increased rapidly at the first beginning, and then gradually remained stable as it further increased, indicating no more Y(III) were adsorbed by (TODGA+1-dodecanol)/SiO_2–P–F600 adsorbent, for instance adsorption saturated. Next, in comparison with other numerous isotherms models, it is well known that Langmuir, Freundlich and Dubinin-Radushkevich isotherm models were most widely used to describe the single-solute adsorption [26]. Here, they were selected to analyze the obtained experimental data and their expressions were described as follows:

$$\text{Langmuir } q_e = \frac{q_{max} b C_e}{1 + bC_e} \quad (7)$$

$$\text{Freundlich } q_e = K_f C_e^{(1/n_f)} \quad (8)$$

$$\text{Dubinin – Radushkevich } q_e = q_{max} \exp\left(-\beta\varepsilon^2\right) \quad (9)$$

$$\varepsilon = RTln\left(1 + \frac{1}{C_e}\right) \quad (10)$$

$$E = \frac{1}{\sqrt{2\beta}} \quad (11)$$

where C_e (mmol/L) means the equilibrium concentration of Y(III), q_e (mmol/g) is the amount of Y(III) adsorbed at equilibrium state, q_{max} (mmol/g) is the theoretical maximum of Y(III) adsorbed, and b (L/mmol), K_f (mmol/g) and β (mol^2/kJ^2) are the Langmuir,

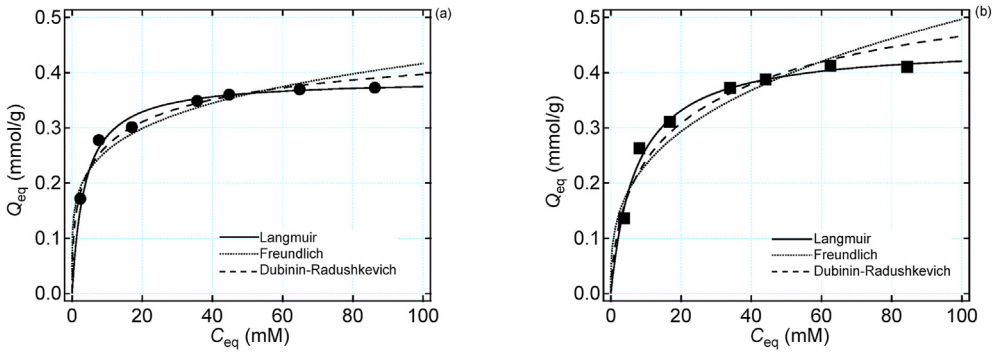

Fig. 5. Non-linear isotherm plots of Y(III) on (TODGA+1-dodecanol)/SiO_2–P–F600 adsorbent at 298 K in (a) HNO_3 solution and (b) HCl solution.

Freundlich and Dubinin-Radushkevich constant, respectively. $1/n_f$ is the Freundlich isotherm exponent constant. *R*, *T* and *E* represent the gas constant (8.314 J/(mol·K)), temperature (K) and the mean adsorption energy (kJ/mol).

Fitting curves and related calculated parameters were shown in Fig. 5 and presented in Table 3, respectively. As it can be seen, higher correlation coefficients were observed for the Langmuir mode ($R^2 > 0.99$) than Freundlich and Dubinin-Radushkevich isotherm model, suggesting that the adsorption process occurred on the monolayer surface of (TODGA+1-dodecanol)/SiO_2–P–F600 adsorbent in HNO_3 and HCl solution rather than a multilayer adsorption or even micropore volume filling [27]. Meanwhile, the theoretical maximum adsorption amount calculated by the Langmuir model were 0.389 mmol/g in HNO_3 solution and 0.451 mmol/g in HCl solution, which was close to their actual adsorption amount as shown in Fig. 5.

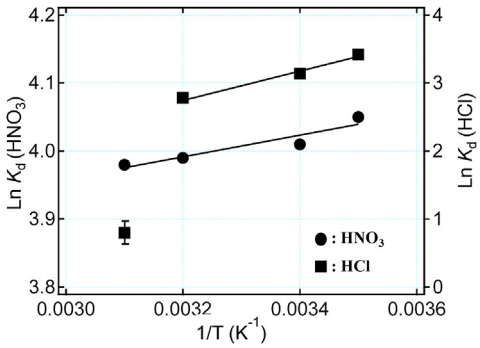

Fig. 6. Effect of solution temperature on the K_d value of Y(III) adsorption onto (TODGA+1-dodecanol)/SiO_2–P–F600 adsorbents.

3.5. Effect of temperature

The effect of temperature on the adsorption of Y(III) by (TODGA+1-dodecanol)/SiO_2–P–F600 adsorbent was carried out at 288, 298, 308 and 323 K in HNO_3 and HCl solution and obtained experimental results were plotted as shown in Fig. 6. It was observed that with increasing the temperature in the solution, the uptake percentages decreased gradually in both acid solutions. In order to make clear the effect of temperature in more details, thermodynamic parameters were calculated by plotting Ln K_d against $1/T$ based on van't Hoff equation as follows [28].

$$LnK_d = -\frac{\Delta H^0}{RT} + \frac{\Delta S^0}{R} \quad (12)$$

Table 3
Calculated parameters for Y(III) adsorption onto (TODGA+1-dodecanol)/SiO_2–P–F600 adsorbent at 298 K.

Models		HNO_3	HCl
Langmuir model parameters	q_{max}	0.389	0.451
	b	0.276	0.139
	R^2	0.999	0.998
Freundlich model parameters	K_f	0.161	0.110
	$1/n_f$	0.206	0.327
	R^2	0.928	0.594
Dubinin-Radushkevich model parameters	q_{max}	0.459	0.596
	E	11.038	8.498
	R^2	0.968	0.939

$$\Delta G^0 = \Delta H^0 - \Delta S^0 T \quad (13)$$

where K_d is distribution coefficient. $\triangle G^0$, $\triangle H^0$, $\triangle S^0$ are the standard changes in Gibbs free energy (J/mol), enthalpy (J/mol), entropy (J/(K·mol)), respectively. R is the universal gas constant (8.314 J/(K·mol)).

ΔH^0 and ΔS^0 could be obtained from the slope and intercept of the fitting lines in Fig. 6, and the theoretical fitting results were summarized as shown in Table 4. It found that all the $\triangle G^0$ values were calculated as negative in the whole temperature range in both HNO_3 and HCl system, which meant the adsorption process happened to be spontaneous and thermodynamically favorable. On the other hand, the degree of $\triangle G^0$ related to the degree of spontaneity, and the gradual decrease in $\triangle G^0$ with increasing temperature suggested that the adsorption process of Y(III) was not more favorable at higher temperature area which was in a good agreement with obtained experimental results. The negative value of $\triangle H^0$ indicated that Y(III) adsorption was exothermic in nature, revealing that high temperature was not beneficial for the adsorption of Y(III) [29]. In addition, the absolute $\triangle H^0$ value in HCl

Table 4
Calculated thermodynamic parameters for Y(III) adsorption onto (TODGA+1-dodecanol)/SiO_2–P–F600 adsorbent.

Temp (K)	ΔG^0 (kJ/mol)		ΔH^0 (kJ/mol)		ΔS^0 (J/mol K)	
	HNO_3	HCl	HNO_3	HCl	HNO_3	HCl
288	−9.66	−26.69	−1.330	−17.33	0.028	0.032
298	−9.95	−27.02				
308	−10.24	−27.34				
323	−10.67	–				

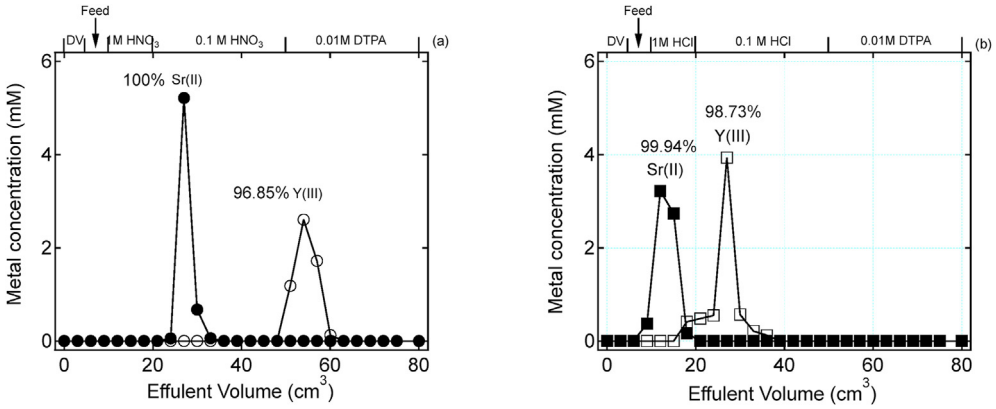

Fig. 7. Column separation results of Sr(II) and Y(III) by using (TODGA+1-dodecanol)/SiO_2–P–F600 adsorbent.

solution was found to be larger than in HNO_3 solution, indicating that the effect of temperate in HCl solution was much more significant.

3.6. Chromatography separation experiments

The column separation experiments between Y(III) and Sr(II) were performed by using (TODGA+1-dodecanol)/SiO_2–P–F600 adsorbent packed column at 298 K in HNO_3 and HCl solution, respectively and results were illustrated as shown in Fig. 7. In the case of HNO_3 solution, with feed solution and 0.1 M HNO_3 flowed through column, Sr(II) quickly leaked out and flowed into the effluent, while Y(III) were still strongly adsorbed onto (TODGA+1-dodecanol)/SiO_2–P–F600 adsorbent and remained into the column, which was consistent with the experiment results obtained in batch experiment (Fig. 4). For instance, (TODGA+1-dodecanol)/SiO_2–P–F600 adsorbent exhibited good affinity towards Y(III) in the whole HNO_3 concentration range than Sr(II). Subsequently, with a supplement of 0.01 M DTPA solution, Y(III) was flowed out with a recovery of 96.85% due to the complexation properties of DTPA was higher than the TODGA ligand in adsorbent. On the other hand, in the case of HCl solution, with feed solution and 1 M HCl solution flowed through column, Sr(II) also quickly leaked out and flowed into the effluent, and Y(III) disassociated with adsorbent and flowed into effluent with adding 0.1 M HCl. This phenomenon was also in a good agreement with batch experimental results shown in Fig. 4. Even though (TODGA+1-dodecanol)/SiO_2–P–F600 adsorbent exhibited weak affinity towards Sr(II) in all the acid range, comparing column separation experimental results, it was found that disassociation rate in HCl solution was relatively faster than in HNO_3 solution. On the other hand, the successful separation of Sr(II) and Y(III) using chromatography separation method was found to be feasible.

4. Conclusion

The adsorption and separation performances of Y(III) by a silica-based TODGA impregnated (TODGA+1-dodecanol)/SiO_2–P–F600 adsorbent were systematically investigated in acid solution under the effect of contact time, acid concentration, solution temperature, adsorption capacity, chromatography etc. Adsorption kinetics were found to fit well with pseudo-second order kinetic model, indicating the adsorption process was dominated by chemisorption. (TODGA+1-dodecanol)/SiO_2–P–F600 exhibited a better affinity towards Y(III) than Sr(II), and the uptake percentages of Y(III) increased gradually with increasing the concentration of acid. Adsorption isotherms fitted well with Langmuir isotherm model, revealing the adsorption process was identified as a monolayer adsorption. Furthermore, with increasing solution temperature, the adsorption performances towards Y(III) decreased, which meant this adsorption process was considered as exothermic in nature, for instance, high temperature was not favorable for the adsorption of Y(III). The chromatography separation experiments of Y(III) from Sr(II)–Y(III) group was successfully completed by elution with 0.01 M DTPA solution in nitric acid system, and 0.1 M HCl solution in hydrochloride system, and this results were also in a good agreement with the experimental results obtained in acid dependence. The results introduced above suggested that the utilization of (TODGA+1-dodecanol)/SiO_2–P–F600 adsorbent to selectively separate of Y(III) from Sr(II)–Y(III) group in both HNO_3 and HCl solution were feasible.

Declaration of competing interest

The authors declare that they have no known competing financial interests or personal relationships that could have appeared to influence the work reported in this paper.

References

[1] A. Pashazadeh, E. de Paiva, N. Mahmoodian, M. Friebe, Calculation of beta radiation dose of a circular Y-90 skin patch: analytical and simulation methods, Radiat. Phys. Chem. 166 (2020) 108491, https://doi.org/10.1016/j.radphyschem.2019.108491.
[2] C. Ince, O. karadeniz, T. Ertay, H. Durak, Collimator and energy window optimization for YTTRIUM-90 bremsstrahlung SPECT imaging, Appl. Radiat. Isot. 167 (2021) 109453, https://doi.org/10.1016/j.apradiso.2020.109453.
[3] G. Sgouros, L. Bodei, M.R. McDevitt, J.R. Nedrow, Radiopharmaceutical therapy in cancer: clinical advances and challenges, Nat. Rev. 19 (2020) 589–608, https://doi.org/10.1038/s41573-020-0073-9.
[4] R. Chakravarty, S. Chakraborty, S. Jadhav, A. Dash, Facile radiochemical separation of clinical-grade 90Y from 90Sr by selective precipitation for targeted radionuclide therapy, Nucl. Med. Biol. 69 (2019) 58–65, https://doi.org/10.1016/j.nucmedbio.2019.01.002.
[5] M.L. Salutsky, H.W. Kirby, Preparation and half life of carrier-free Yttrium-90, Anal. Chem. 27 (1955) 567–569, https://doi.org/10.1021/ac60100a024.
[6] K. Roy, P.K. Mohapatra, N. Rawat, D.K. Pal, S. Basu, V.K. Manchanda, Separation of ^{90}Y from ^{90}Sr using zirconium vanadate as the ion exchanger, Appl. Radiat. Isot. 60 (2004) 621–624. https://doi:10.1016/j.apradiso.2003.09.015.
[7] P. Kandwal, S.A. Ansari, P.K. Mohapatra, V.K. Manchanda, Separation of carrier free ^{90}Y from ^{90}Sr by hollow fiber supported liquid membrane containing bis(2-ethylhexyl) phosphonic acid, Separ. Sci. Technol. 46 (2011) 904–911, https://doi.org/10.1080/01496395.2010.541402.
[8] M. Hemmati, M. Rajabi, A. Asghari, Magnetic nanoparticle based solid-phase extraction of heavy metal ions: a review on recent advances, Microchim. Acta 185 (2018) 160, https://doi.org/10.1007/s00604-018-2670-4.
[9] N.K. Soliman, A.F. Moustafa, Industrial solid waste for heavy metals adsorption features and challenges; a review, J. Mater. Res. Technol. 9 (2020) 10235–10253, https://doi.org/10.1016/j.jmrt.2020.07.045.
[10] W.J. Mu, Q.H. Yu, J.Y. Gu, X.L. Li, Y.C. Yang, H.Y. Wei, S.M. Peng, Bonding of crown ethers to α-zirconium phosphate—novel layered adsorbent for

radioactive strontium separation, Separ. Purif. Technol. 240 (2020) 116658, https://doi.org/10.1016/j.seppur.2020.116658.
[11] T. Kawamura, T. Ito, S.Y. Kim, Adsorption and separation behavior of strontium and yttrium using a silica-based CMPO adsorbent, J. Radioanal. Nucl. Chem. 320 (2019) 9–14, https://doi.org/10.1007/s10967-019-06446-4.
[12] F. Gritti, G. Guiochon, Adsorption mechanism in RPLC. Effect of the nature of the organic modifier, Anal. Chem. 77 (2005) 4257–4272, https://doi.org/10.1021/ac0580058.
[13] Y. Wu, C.P. Lee, H. Mimura, X.X. Zhang, Y.Z. Wei, Stable solidification of silica-based ammonium molybdophosphate by allophane: application to treatment of radioactive cesium in secondary solid wastes generated from fukushima, J. Hazard Mater. 341 (2018) 46–54, https://doi.org/10.1016/j.jhazmat.2017.07.044.
[14] Y. Wu, S.Y. Kim, D. Tozawa, T. Ito, T. Tada, K. Hitomi, E. Kuraoka, H. Yamazaki, K. Ishii, Equilibrium and kinetic studies of selective adsorption and separation for strontium using DtBuCH18C6 loaded resin, J. Nucl. Sci. Technol. 49 (2012) 320–327, https://doi.org/10.1080/00223131.2012.660022.
[15] W. Zhang, S.Q. Yu, S.C. Zhang, J. Zhou, S.Y. Ning, X.P. Wang, Y.Z. Wei, Separation of scandium from the other rare earth elements with a novel macroporous silica-polymer based adsorbent HDEHP/SiO_2-P, Hydrometallurgy 185 (2019) 117–124, https://doi.org/10.1016/j.hydromet.2019.01.012.
[16] S.Y. Ning, S.C. Zhang, W. Zhang, J. Zhou, S.Y. Wang, X.P. Wang, Y.Z. Wei, Separation and recovery of Rh, Ru and Pd from nitrate solution with a silica based IsoBu-BTP/SiO_2-P adsorbent, Hydrometallurgy 191 (2020) 105207, https://doi.org/10.1016/j.hydromet.2019.105207.
[17] L. Chaabane, E. Beyou, A.E. Ghali, M.H.V. Baouab, Comparative studies on the adsorption of metal ions from aqueous solutions using various functionalized graphene oxide sheets as supported adsorbents, J. Hazard Mater. 389 (2020) 121839, https://doi.org/10.1016/j.jhazmat.2019.121839.
[18] S. Sahu, L. Mallik, S. Pahi, B. Barik, U.K. Sahu, M. Sillanpaa, R.K. Patel, Facile synthesis of poly o-toluidine modified lanthanum phosphate nanocomposite as a superior adsorbent for selective fluoride removal: a mechanistic and kinetic study, Chemosphere 252 (2020) 126551, https://doi.org/10.1016/j.chemosphere.2020.126551.
[19] Y. Wu, X.X. Zhang, S.Y. Kim, Y.Z. Wei, Simultaneous separation and recovery of Cs(I) and Sr(II) using a hybrid macrocyclic compounds loaded adsorbent. Kinetic, equilibrium and dynamic adsorption studies, J. Nucl. Sci. Technol. 53 (2016) 1968–1977, https://doi.org/10.1080/00223131.2016.1175979.
[20] S.A. Ansari, P.N. Pathak, V.K. Manchanda, M. Husain, A.K. Prasad, V.S. Parmar, N,N,N′,N′-Tetraoctyl Diglycolamide (TODGA): A promising extractant for actinide-partitioning from high-level waste (HLW), Solvent Extr. Ion Exch. 23 (2005) 463–479, https://doi.org/10.1081/SEI-200066296.
[21] A.M. Alasadi, F.I. Khaili, A.M. Awwad, Adsorption of Cu(II), Ni(II) and Zn(II) ions by nano kaolinite: thermodynamics and kinetics studies, Chem. Int. 5 (2019) 258–268, https://doi.org/10.5281/zenodo.2644985.
[22] M.A. Hubbe, S. Azizian, S. Douven, Implications of apparent pseudo-second-order adsorption kinetics onto cellulosic materials: a review, Bioresources 14 (2019) 7582–7626.
[23] S. Dutta, P.K. Mohapatra, V.K. Manchanda, Separation of ^{90}Y from ^{90}Sr by a solvent extraction method using *N,N,N′,N′*–tetraoctyl diglycolamide (TODGA) as the extractant, Appl. Radiat. Isot. 69 (2011) 158–162, https://doi.org/10.1016/j.apradiso.2010.09.016.
[24] P.N. Pathak, S.A. Ansari, S. Kumar, B.S. Tomar, V.K. Manchanda, Dynamic light scattering study on the aggregation behaviour of *N,N,N′,N′*-tetraoctyl diglycolamide (TODGA) and its correlation with the extraction behavior of metal ions, J. Colloid Interface Sci. 342 (2010) 114–118, https://doi.org/10.1016/j.jcis.2009.10.015.
[25] D.M. Brigham, A.S. Ivanov, B.A. Moyer, L.H. Delmau, V.S. Bryantsev, R.J. Ellis, Trefoil-shaped outer-sphere ion clusters mediate lanthanide(III) ion transport with diglycolamide ligands, J. Am. Chem. Soc. 139 (2017) 17350–17358, https://doi.org/10.1021/jacs.7b07318.
[26] N. Can, B.C. Omur, A. Altindal, Modeling of heavy metal ion adsorption isotherms onto metallophthalocyanine film, Sensor. Actuator. B Chem. 237 (2016) 953–961, https://doi.org/10.1016/j.snb.2016.07.026.
[27] P.A. Milani, K.B. Debs, G. Labuto, E.N. Vasconcelos, Martins Carrilho Agricultural solid waste for sorption of metal ions: part I—characterization and use of lettuce roots and sugarcane bagasse for Cu(II), Fe(II), Zn(II), and Mn(II) sorption from aqueous medium, Environ. Sci. Pollut. Res. 25 (2018) 35895–35905, https://doi.org/10.1007/s11356-018-1615-0.
[28] M. Sharma, J. Singh, S. Hazra, S. Basu, Adsorption of heavy metal ions by mesoporous ZnO and TiO2@ZnO monoliths: adsorption and kinetic studies, Microchem. J. 145 (2019) 105–112, https://doi.org/10.1016/j.microc.2018.10.026.
[29] L. Li, W. Lu, D.X. Ding, Z.R. Dai, C. Cao, L. Liu, T. Chen, Adsorption properties of pyrene-functionalized nano-Fe_3O_4 mesoporous materials for uranium, J. Solid State Chem. 27 (2019) 666–673, https://doi.org/10.1016/j.jssc.2018.12.030.